Acta Mechanica 118, 55–64 (1996)

ACTA MECHANICA


# Mixed convection in non-Newtonian fluids along a vertical plate in a porous medium

**R. S. R. Gorla,** Cleveland, Ohio, and **M. Kumari,** Bangalore, India

(Received June 14, 1995)

**Summary.** The problem of mixed convection from vertical surfaces in a porous medium saturated with a power-law type non-Newtonian fluid is investigated. The transformed conservation laws are solved numerically for the case of variable wall temperature conditions. Results for the details of the velocity and temperature fields as well as the Nusselt number have been presented. The viscosity index ranged from 0.5–2.0.

## Notation

| | |
|---|---|
| $d$ | particle diameter |
| $f$ | dimensionless stream function |
| $g$ | acceleration due to gravity |
| $h$ | heat transfer coefficient |
| $k$ | thermal conductivity |
| $K$ | permeability coefficient of the porous medium |
| $L$ | length of the plate |
| $n$ | viscosity index |
| Nu | Nusselt number |
| Pe | Peclet number |
| Pr | Prandtl number |
| $q_w$ | wall heat flux |
| Ra | Rayleigh number |
| Re | Reynolds number |
| $T$ | temperature |
| $u, v$ | velocity components in $x$ and $y$ directions |
| $x, y$ | axial and normal coordinates |
| $\alpha$ | thermal diffusivity |
| $\beta$ | coefficient of thermal expansion |
| $\eta$ | dimensionless distance |
| $\Theta$ | dimensionless temperature |
| $\mu$ | dynamic viscosity |
| $\varrho$ | density |
| $\varepsilon$ | porosity |
| $\chi$ | mixed convection nonsimilar parameter |
| $\psi$ | stream function |

*Subscripts*

| | |
|---|---|
| $w$ | surface conditions |
| $\infty$ | conditions far away from the surface |

## 1 Introduction

Convective heat transfer in porous media has received considerable interest because of numerous thermal engineering applications in several areas such as geothermal engineering, thermal insulation systems, petroleum recovery, filtration processes, packed bed reactors, sensible heat storage beds, ceramic processing and ground water pollution.

Similarity solutions for free convective heat transfer from a vertical plate in a fluid-saturated porous media were obtained by Cheng and Minkowycz [1]. Gorla and co-workers [2], [3] developed a procedure to investigate the nonsimilar boundary layer problem of free convection from a vertical plate embedded in a porous medium with an arbitrarily varying surface temperature or heat flux. The problem of mixed convection from surfaces embedded in porous media was studied by Minkowycz et al. [4] as well as Ranganathan and Viskanta [5]. Hsieh et al. [6] presented nonsimilar solutions for mixed convection in porous media. All these studies were concerned with Newtonian fluid flows. A number of industrially important fluids including fossil fuels which may saturate underground beds display non-Newtonian fluid behavior. Non-Newtonian fluids exhibit a nonlinear relationship between shear stress and shear rate.

Chen and Chen [7] and Mehta and Rao [8] presented similarity solutions for free convection of non-Newtonian fluids over vertical surfaces in porous media. Nakayama and Koyama [9] studied the natural convection over a non-isothermal body of arbitrary geometry placed in a porous medium. A similarity solution was derived by Mehta and Rao [10] for the natural convective boundary layer flow of a non-Newtonian fluid over a non-isothermal horizontal plate immersed in a porous medium. The problem of mixed convection from vertical surfaces in porous media saturated with non-Newtonian fluids has not been investigated.

The present work has been undertaken in order to analyze the problem of nonsimilar mixed convection from a vertical non-isothermal flat plate embedded in non-Newtonian fluid-saturated porous media. The boundary condition of variable surface temperature is treated in this paper. The power law model of Ostwald-de-Waele which is adequate for many non-Newtonian fluids will be considered here. The transformed boundary layer equations are solved using a finite difference method. The numerical results for the velocity and temperature fields are obtained.

## 2 Governing equations

Let us consider the combined convection flow in a porous medium saturated with a non-Newtonian fluid along a heat vertical impermeable flat plate. The flow model is shown in Fig. 1. The axial and normal coordinates are $x$ and $y$. The gravitational acceleration $g$ is in the direction

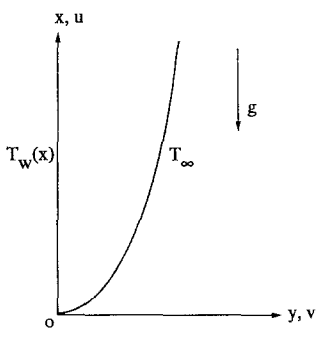


**Fig. 1.** Coordinate system and flow model

opposite to the $x$ coordinate. The surface of the plate is maintained at a temperature of $T_w(x)$. The flow velocity and the pores of the porous medium are assumed to be small and therefore Darcy's model is assumed to be valid. The governing equations under Boussinesq and boundary layer approximation may be written as:

$$\frac{\partial u}{\partial x} + \frac{\partial v}{\partial y} = 0, \tag{1}$$

$$u^n = U_\infty^n + \frac{K}{\mu}[\varrho g \beta (T - T_\infty)], \tag{2}$$

$$u\frac{\partial T}{\partial x} + v\frac{\partial T}{\partial y} = \alpha \frac{\partial^2 T}{\partial y^2}. \tag{3}$$

In the above equations, $u$ and $v$ are the Darcian velocity components in $x$ and $y$ directions; $U_\infty$ the free-stream velocity; $T$ the temperature; $n$ the viscosity index; $\varrho$ the density; $\mu$ the viscosity; $\beta$ the volumetric coefficient of expansion; $K$ the permeability of the porous medium and $\alpha$ the equivalent thermal diffusivity of the porous medium.

For the power law model of Ostwald-de-Waele, Christopher and Middleman [11] and Dharmadhikari and Kale [12] proposed the following relationships for the permeability:

$$K = \begin{cases} \dfrac{6}{25}\left(\dfrac{n\varepsilon}{3n+1}\right)^n \left[\dfrac{\varepsilon d}{3(1-\varepsilon)}\right]^{n+1} & [11] \\ \dfrac{2}{\varepsilon}\left[\dfrac{d\varepsilon^2}{8(1-\varepsilon)}\right]^{n+1} \left(\dfrac{6n+1}{10n-3}\right)\left(\dfrac{16}{75}\right)^{3(10n-3)/(10n+11)} & [12] \end{cases} \tag{4}$$

In the above equation, $d$ is the particle diameter and $\varepsilon$ the porosity.

The appropriate boundary conditions are given by

$$\begin{aligned} &y = 0: \quad v = 0, \quad T = T_\infty + ax^\lambda, \\ &y \to \infty: \quad u = U_\infty, \quad T = T_\infty \end{aligned} \tag{5}$$

where $a$ and $\lambda$ are constants. We note that $\lambda = 0$ corresponds to isothermal wall conditions.

The continuity equation is automatically satisfied by defining a stream function $\psi(x, y)$ such that

$$u = \frac{\partial \psi}{\partial y} \quad \text{and} \quad v = -\frac{\partial \psi}{\partial x}. \tag{6}$$

Proceeding with the analysis, we define the following transformations:

$$\begin{aligned} \eta &= \left(\frac{y}{x}\right)\frac{\sqrt{\mathrm{Pe}_x}}{\chi}, \\ \chi^{-1} &= 1 + \sqrt{\frac{\mathrm{Ra}_x}{\mathrm{Pe}_x}}, \\ \psi &= \alpha \frac{\sqrt{\mathrm{Pe}_x}}{\chi} f(\chi, \eta), \end{aligned} \tag{7}$$

$$\theta = \frac{T - T_\infty}{T_w - T_\infty},$$

$$\mathrm{Pe}_x = \frac{U_\infty x}{\alpha}, \tag{7}$$

$$\mathrm{Ra}_x = \frac{x}{\alpha}\left[\frac{\varrho k g \beta (T_w - T_\infty)}{\mu}\right]^{1/n}.$$

Substituting the expressions in (7) into Eqs. (2), (3) and (5), the transformed governing equations may be written as

$$n(f')^{n-1} f'' = (1-\chi)^{2n}\,\theta' \tag{8}$$

$$\theta'' + \frac{1}{2}\left[1 + \frac{\lambda}{n}(1-\chi)\right] f\theta' - \lambda f'\theta = \frac{\lambda}{2n}\chi(1-\chi)\left[\theta'\frac{\partial f}{\partial \chi} - f'\frac{\partial \theta}{\partial \chi}\right], \tag{9}$$

$$\left[1 + \frac{\lambda}{n}(1-\chi)\right] f(\chi, 0) - \frac{\lambda}{n}\chi(1-\chi)\frac{\partial f}{\partial \chi}(\chi, 0) = 0,$$

$$\theta(\chi, 0) = 1, \tag{10}$$

$$f'(\chi, \infty) = \chi^2, \quad \theta(\chi, \infty) = 0.$$

Primes in the above equations denote partial differentiation with respect to $\eta$. We note that $\chi = 0$ and 1 correspond to pure free and forced convection cases, respectively.

For practical applications, it is usually the velocity components, friction factor and Nusselt number that are of interest. These are given by

$$u = \frac{U_\infty}{\chi^2} f'(\chi, \eta),$$

$$v = -\frac{\alpha\sqrt{\mathrm{Pe}_x}}{2x}\left[\frac{1}{\chi} f + \left(\frac{1-\chi}{\chi}\right)\left(\frac{\lambda}{n}\right) f + (\chi - 1)\left(\frac{\lambda}{n}\right)\frac{\partial f}{\partial \chi} - f'\eta\left[\frac{1}{\chi} + \left(\frac{\chi - 1}{\chi}\right)\left(\frac{\lambda}{n}\right)\right]\right],$$

$$C_{fx} = \frac{2\tau_w}{\varrho U_\infty^2} = \frac{2}{\mathrm{Re}_x}(\chi^{-3n})\,\mathrm{Pe}_x^{n/2}\,[f''(\chi, 0)]^n, \tag{11}$$

$$\mathrm{Nu}_x = -\frac{\sqrt{\mathrm{Pe}_x}}{\chi}\theta'(\chi, 0).$$

## 3 Numerical scheme

The numerical scheme to solve Eqs. (8) and (9) adopted here is based on a combination of the following concepts:

(a) The boundary conditions for $\eta = \infty$ is replaced by

$$f'(\chi, \eta_{\max}) = \chi^2, \quad \theta(\chi, \eta_{\max}) = 0 \tag{12}$$

where $\eta_{\max}$ is sufficiently large value of $\eta$ where the boundary condition (12) for velocity is satisfied. $\eta_{\max}$ varies with the value of $\eta$. We have set $\eta_{\max} = 25$ in the present work.

(b) The two-dimensional domain of interest, $(\chi, \eta)$ is discretized with an equispaced mesh in the $\chi$ direction and another equispaced mesh in the $\eta$ direction.

(c) The partial derivatives with respect to $\chi$ and $\eta$ are all evaluated by the central difference approximations. The central difference approximation for the partial derivatives with respect to $\chi$ vanish when $\chi = 0$ and $\chi = 1$ which correspond to the first and the last mesh points on the $\chi$ axis, or free and forced convection, respectively.

(d) Two iteration loops based on the successive substitution are used because of the nonlinearity of the equations.

(e) In each inner iteration loop, the value of $\chi$ is fixed while each of Eqs. (8) and (9) is solved as a linear second-order boundary value problem of ODE on the $\eta$ domain. The inner iteration is continued until the nonlinear solution converges for the fixed value of $\chi$.

(f) In the outer iteration loop, the value of $\chi$ is advanced from 0 to 1. The derivatives with respect to $\chi$ are updated after every outer iteration step.

More details of the numerical solution scheme are explained in the remainder of this section.

In an inner iterations step, the finite difference approximation for each of the Eqs. (8) and (9) is solved as a boundary value problem. To describe the procedure, we consider Eq. (8) first. By defining

$$U = f. \tag{13}$$

Eq. (8) may be written in the form

$$a_1 U'' = s_1 \tag{14}$$

where

$$\begin{aligned} a_1 &= n\,|U'|^{n-1}, \\ s_1 &= (1-\chi)^{2n}\,\theta'. \end{aligned} \tag{15}$$

The boundary conditions for $U$ are

$$U(\chi, 0) = 0, \quad U'(\chi, \eta_{\max}) = \chi^2. \tag{16}$$

Note that we replace the boundary condition at infinity by that at a finite distance $\eta_{\max}$.

The coefficient $a_1$ and the source terms in Eq. (14) in the inner iteration step are evaluated using the solution from the previous iteration step. Equation (14) is then transformed to a finite difference equation by applying the central difference approximations to the first and second derivatives. The finite difference equations form a tridiagonal system and can be solved by the tridiagonal solution scheme.

Equation (9) is also written as a second-order boundary value problem similar to Eq. (14), namely

$$a_2\theta'' + b_2\theta' + c_2\theta = s_2, \tag{17}$$

$$\begin{aligned} a_2 &= 1, \\ b_2 &= U\left[\frac{1}{2} + \frac{\lambda}{2n}(1-\chi)\right], \\ c_2 &= -U'\lambda, \\ s_2 &= \frac{\lambda}{2n}\chi(\chi-1)\left[U'\frac{\partial\theta}{\partial\chi} - \theta'\frac{\partial U}{\partial\chi}\right]. \end{aligned} \tag{18}$$

The numerical results are affected by the number of mesh points in both directions. To obtain accurate results, a mesh sensitivity study was performed. In the $\eta$ direction, after the results for the mesh points of 51, 100, 200, and 800 were compared it was found that 200 points give the same results as 800. In the $\chi$ direction, only 11 mesh points were found to give as accurate results as with 21 points. Therefore, the remainder of the computations were performed with 200 times 11 mesh points.

## 4 Results and discussion

Numerical data for the missing wall gradient $-\Theta'(\chi, 0)$ are presented for $\chi$ ranging from $0-1$ in Tables $1-6$. We have chosen $\lambda$ and $n$ as prescribable parameters. To assess the accuracy of the present results, we have shown a comparison of our results with those of Hsieh et al. [6] for the case of Newtonian fluid, namely, $n = 1$. It may be noted that the agreement between our results and the literature values is within $2-5\%$ difference. We therefore conclude that our results are very accurate.

**Table 1.** Comparison of values of $-\theta'(\chi, 0)$ for $n = 1.0$

| $-\theta'(\chi, 0)$ | | | | |
|---|---|---|---|---|
| | Present results | | Hsieh et al. | |
| $\chi$ | $\lambda = 0.0$ | $\lambda = 0.5$ | $\lambda = 0.0$ | $\lambda = 0.5$ |
| 1.0 | 0.56414 | 0.88601 | 0.5642 | 0.8862 |
| 0.9 | 0.51028 | 0.80144 | 0.5098 | 0.8014 |
| 0.8 | 0.46201 | 0.72637 | 0.4603 | 0.7259 |
| 0.7 | 0.42148 | 0.66417 | 0.4174 | 0.6629 |
| 0.6 | 0.39092 | 0.61883 | 0.3832 | 0.6160 |
| 0.5 | 0.37207 | 0.59411 | 0.3603 | 0.5890 |
| 0.4 | 0.36569 | 0.59202 | 0.3506 | 0.5844 |
| 0.3 | 0.37165 | 0.61195 | 0.3550 | 0.6026 |
| 0.2 | 0.38913 | 0.65136 | 0.3732 | 0.6419 |
| 0.1 | 0.41698 | 0.70701 | 0.4035 | 0.6991 |
| 0.0 | 0.45383 | 0.77584 | 0.4438 | 0.7704 |

**Table 2.** Values of $-\theta'(\chi, 0)$ for $n = 0.5$

| $-\theta'(\chi, 0)$ | | | | |
|---|---|---|---|---|
| $\chi$ | $\lambda = 0.0$ | $\lambda = 0.5$ | $\lambda = 1.0$ | $\lambda = 2.0$ |
| 1.0 | 0.56414 | 0.93070 | 1.12812 | 1.50420 |
| 0.9 | 0.54405 | 0.91541 | 1.10565 | 1.47647 |
| 0.8 | 0.52441 | 0.90108 | 1.08342 | 1.44901 |
| 0.7 | 0.50537 | 0.88778 | 1.06150 | 1.42187 |
| 0.6 | 0.48708 | 0.87556 | 1.03997 | 1.39513 |
| 0.5 | 0.46968 | 0.86445 | 1.01902 | 1.36897 |
| 0.4 | 0.45329 | 0.85444 | 0.99892 | 1.34368 |
| 0.3 | 0.43799 | 0.84551 | 0.98018 | 1.31992 |
| 0.2 | 0.42381 | 0.83760 | 0.96322 | 1.29839 |
| 0.1 | 0.41075 | 0.83051 | 0.94886 | 1.28106 |
| 0.0 | 0.40692 | 0.85862 | 0.94949 | 1.27807 |

**Table 3.** Values of $-\theta'(\chi, 0)$ for $n = 0.8$

| $-\theta'(\chi, 0)$ | | | | |
|---|---|---|---|---|
| $\chi$ | $\lambda = 0.0$ | $\lambda = 0.5$ | $\lambda = 1.0$ | $\lambda = 2.0$ |
| 1.0 | 0.56414 | 0.88601 | 1.12796 | 1.50391 |
| 0.9 | 0.51424 | 0.80902 | 1.03026 | 1.37402 |
| 0.8 | 0.47221 | 0.74604 | 0.95079 | 1.26885 |
| 0.7 | 0.43772 | 0.69587 | 0.88782 | 1.18595 |
| 0.6 | 0.41127 | 0.65919 | 0.84198 | 1.12605 |
| 0.5 | 0.39326 | 0.63694 | 0.81443 | 1.09045 |
| 0.4 | 0.38387 | 0.62999 | 0.80653 | 1.08080 |
| 0.3 | 0.38314 | 0.63843 | 0.81895 | 1.09826 |
| 0.2 | 0.39118 | 0.66218 | 0.85190 | 1.14385 |
| 0.1 | 0.40844 | 0.70133 | 0.90542 | 1.21806 |
| 0.0 | 0.43927 | 0.76178 | 0.98489 | 1.32547 |

**Table 4.** Values of $-\theta'(\chi, 0)$ for $n = 1.0$

| $-\theta'(\chi, 0)$ | | | | |
|---|---|---|---|---|
| $\chi$ | $\lambda = 0.0$ | $\lambda = 0.5$ | $\lambda = 1.0$ | $\lambda = 2.0$ |
| 1.0 | 0.56414 | 0.88601 | 1.12812 | 1.50404 |
| 0.9 | 0.51028 | 0.80144 | 1.02045 | 1.36052 |
| 0.8 | 0.46201 | 0.72637 | 0.92510 | 1.23361 |
| 0.7 | 0.42148 | 0.66417 | 0.84632 | 1.12889 |
| 0.6 | 0.39092 | 0.61883 | 0.78916 | 1.05290 |
| 0.5 | 0.37207 | 0.59411 | 0.75854 | 1.01203 |
| 0.4 | 0.36569 | 0.59202 | 0.75747 | 1.01058 |
| 0.3 | 0.37165 | 0.61195 | 0.78546 | 1.04887 |
| 0.2 | 0.38913 | 0.65136 | 0.83899 | 1.12280 |
| 0.1 | 0.41698 | 0.70701 | 0.91339 | 1.22558 |
| 0.0 | 0.45383 | 0.77584 | 1.00426 | 1.35033 |

**Table 5.** Values of $-\theta'(\chi, 0)$ for $n = 1.5$

| $-\theta'(\chi, 0)$ | | | | |
|---|---|---|---|---|
| $\chi$ | $\lambda = 0.0$ | $\lambda = 0.5$ | $\lambda = 1.0$ | $\lambda = 2.0$ |
| 1.0 | 0.56414 | 0.88601 | 1.12796 | 1.50391 |
| 0.9 | 0.50846 | 0.79796 | 1.01564 | 1.35414 |
| 0.8 | 0.45479 | 0.71245 | 0.90636 | 1.20840 |
| 0.7 | 0.40631 | 0.63447 | 0.80632 | 1.07499 |
| 0.6 | 0.36821 | 0.57348 | 0.72747 | 0.96979 |
| 0.5 | 0.34682 | 0.54268 | 0.68737 | 0.91615 |
| 0.4 | 0.34613 | 0.55033 | 0.69825 | 0.93104 |
| 0.3 | 0.36464 | 0.59167 | 0.75429 | 1.00777 |
| 0.2 | 0.39689 | 0.65345 | 0.83707 | 1.12112 |
| 0.1 | 0.43712 | 0.72645 | 0.93366 | 1.25276 |
| 0.0 | 0.48134 | 0.80415 | 1.03548 | 1.39064 |

**Table 6.** Values of $-\theta'(\chi, 0)$ for $n = 2.0$

| $-\theta'(\chi, 0)$ | | | | |
|---|---|---|---|---|
| $\chi$ | $\lambda = 0.0$ | $\lambda = 0.5$ | $\lambda = 1.0$ | $\lambda = 2.0$ |
| 1.0 | 0.56666 | 0.88638 | 1.12812 | 1.50404 |
| 0.9 | 0.51325 | 0.79837 | 1.01553 | 1.35378 |
| 0.8 | 0.46246 | 0.71145 | 0.90373 | 1.20438 |
| 0.7 | 0.41647 | 0.62872 | 0.79625 | 1.06029 |
| 0.6 | 0.37971 | 0.55969 | 0.70507 | 0.93718 |
| 0.5 | 0.36003 | 0.52496 | 0.65829 | 0.87287 |
| 0.4 | 0.36406 | 0.54093 | 0.68037 | 0.90257 |
| 0.3 | 0.38807 | 0.59489 | 0.75393 | 1.00394 |
| 0.2 | 0.42314 | 0.66594 | 0.84922 | 1.13473 |
| 0.1 | 0.46371 | 0.74295 | 0.95122 | 1.27383 |
| 0.0 | 0.50698 | 0.82209 | 1.05505 | 1.41437 |

Figures 2–4 display results for the velocity and temperature profiles. We have treated the viscosity index $n$, combined convection parameter $\chi$ and the temperature power law exponent $\lambda$ as parameters. We note that $\chi = 0$ and 1 represent pure natural convection and forced convection, respectively. As $\chi$ increases, we note that the momentum boundary layer thickness increases. As $\lambda$ increases, the momentum and thermal boundary layer thicknesses decrease. We note that $\lambda = 0$ corresponds to isothermal boundary condition. The velocity at the porous wall

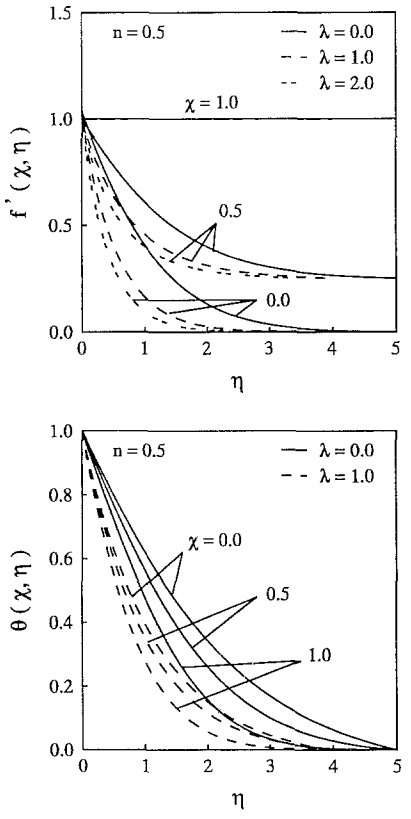


Fig. 2

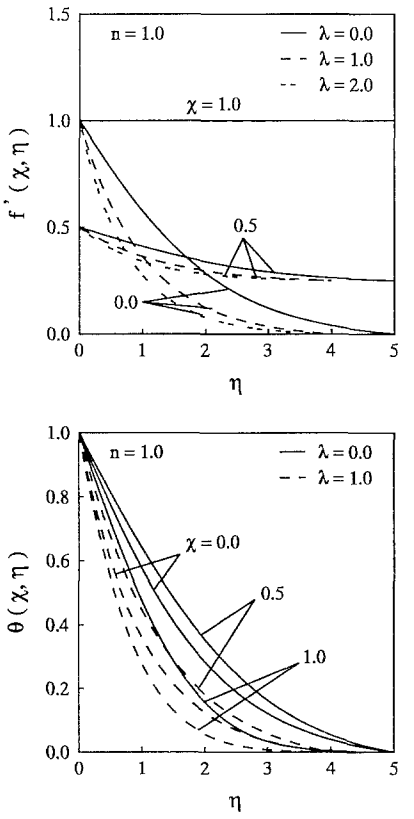


Fig. 3

**Figs. 2, 3.** Velocity and temperature profiles (**Fig. 2** $n = 0.5$), (**Fig. 3** $n = 1$)

decreases with $\chi$ and $n$. As $\lambda$ increases, the wall temperature gradient increases and therefore the surface heat transfer increases.

Figures 5 – 7 display the variation of the local heat transfer rate (Nusselt number) with $\chi$. As $\chi$ varies from 0 to 1, the heat transfer rate decreases initially, reaches a minimum and then increases as $\chi$ approaches 1. For $n = 0.5$, the Nusselt number tends to vary with $\chi$ in a linear fashion. The heat transfer rate for pure forced convection ($\chi = 1$) is greater than that for pure free

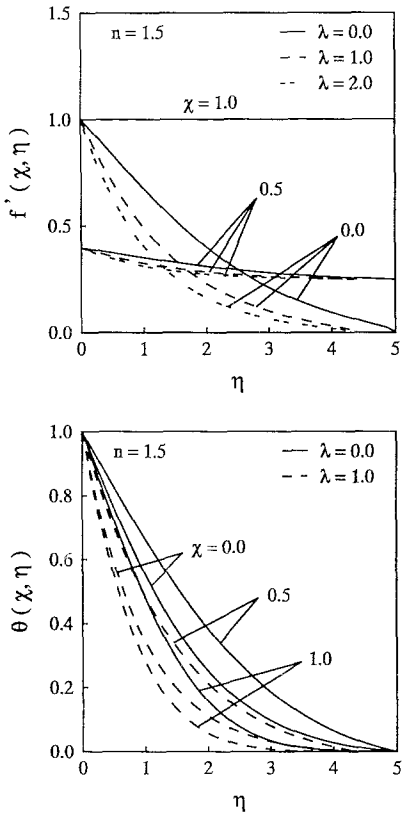


**Fig. 4.** Velocity and temperature profiles ($n = 1.5$)

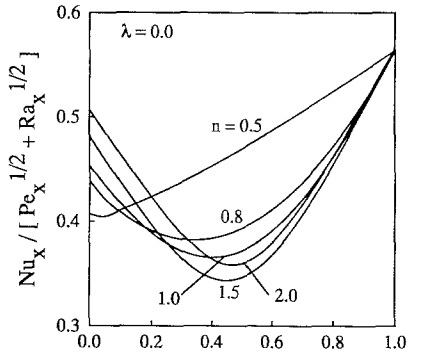


**Fig. 5**

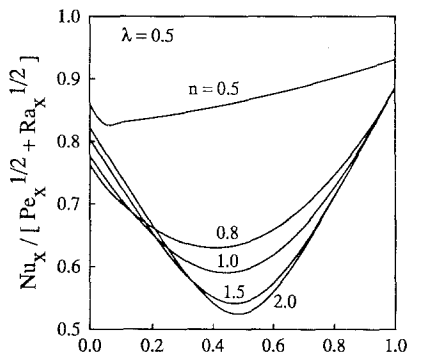


**Fig. 6**

**Figs. 5, 6.** Local Nusselt number versus $\chi$ (**Fig. 5** $\lambda = 0.0$), (**Fig. 6** $\lambda = 0.5$)

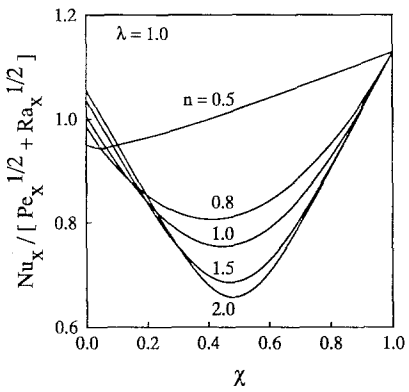


**Fig. 7**

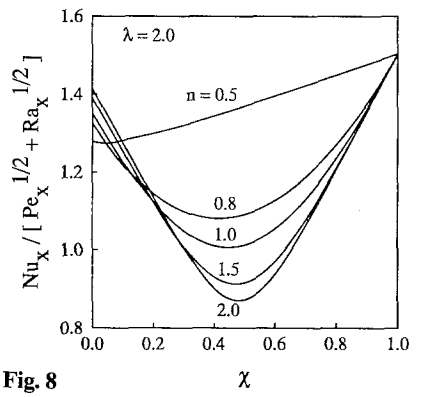


**Fig. 8**

**Figs. 7, 8.** Local Nusselt number versus $\chi$ (**Fig. 7** $\lambda = 1.0$), (**Fig. 8** $\lambda = 2.0$)

convection ($\chi = 0$) case. As $n$ increases, the Nusselt number tends to decrease. This indicates that pseudoplastic ($n < 1$) fluids are associated with higher heat transfer rates when compared to dilatant ($n > 1$) fluids. As $\lambda$ increases, the Nusselt number increases, thus, indicating that nonisothermal surfaces are associated with higher heat transfer rates than isothermal surfaces.

## 5 Concluding remarks

In this paper, we have presented a boundary layer analysis for the problem of combined convection from a vertical surface with variable wall temperature and embedded in a porous medium saturated with Ostwald-de-Waele type non-Newtonian fluid. The nonsimilar parameter $\chi$ is introduced and as $\chi$ varies from 0 to 1, the entire regime of the mixed convection case is described. The nonsimilar boundary layer equations are solved numerically by means of a finite difference scheme. It is observed that pseudoplastic fluids display augmented surface heat transfer rates when compared to Newtonian fluids. This fact may be helpful in choosing a proper fluid for a given practical application.

## References

[1] Cheng, P., Minkowycz, W. J.: Free convection about a vertical plate embedded in a porous medium with application to heat transfer from a dike. J. Geophys. Res. **82,** 2040–2044 (1977).
[2] Gorla, R. S. R., Zinalabedini, A. H.: Free convection from a vertical plate with nonuniform surface temperature and embedded in a porous medium. Trans. ASME J. Energy Res. Techn. **109,** 26–30 (1987).
[3] Gorla, R. S. R., Tornabene, R.: Free convection from a vertical plate with nonuniform surface heat flux and embedded in a porous medium. Trans. Porous Media J. **3,** 95–106 (1988).
[4] Minkowycz, W. J., Cheng, P., Chang, C. H.: Mixed convection about a nonisothermal cylinder and sphere in a porous medium. Numer. Heat Transfer **8,** 349–359 (1985).
[5] Ranganathan, P., Viskanta, R.: Mixed convection boundary layer flow along a vertical surface in a porous medium. Numer. Heat Transfer **7,** 305–317 (1984).
[6] Hsieh, J. C., Chen, T. S., Armaly, B. F.: Nonsimilarity solutions for mixed convection from vertical surfaces in porous media. Int. J. Heat Mass Transfer **36,** 1485–1493 (1993).
[7] Chen, H. T., Chen, C. K.: Natural convection of non-Newtonian fluids about a horizontal surface in a porous medium. Trans. ASME J. Energy Res. Techn. **109,** 119–123 (1987).
[8] Mehta, K. N., Rao, K. N.: Buoyancy-induced flow of non-Newtonian fluids in a porous medium past a vertical plate with nonuniform surface heat flux. Int. J. Eng. Sci. **32,** 297–302 (1994).
[9] Nakayama, A., Koyama, H.: Buoyancy-induced flow of non-Newtonian fluids over a non-isothermal body of arbitrary shape in a fluid-saturated porous medium. Appl. Sci. Res. **48,** 55–70 (1991).
[10] Mehta, K. N., Rao, K. N.: Buoyancy-induced flow of non-Newtonian fluids over a non-isothermal horizontal plate embedded in a porous medium. Int. J. Eng. Sci. **32,** 521–525 (1994).
[11] Christopher, R. H., Middleman, S.: Power-law flow through a packed tube. I & EC Fundamentals **4,** 422–426 (1965).
[12] Dharmadhikari, R. V., Kale, D. D.: Flow of non-Newtonian fluids through porous media. Chem. Eng. Sci. **40,** 527–529 (1985).

**Authors' addresses:** Dr. Rama Subba Reddy Gorla, Department of Mechanical Engineering, Cleveland State University Cleveland, Ohio 44115, U.S.A., and Dr. M. Kumari, Department of Mathematics, Indian Institute of Science, Bangalore 560012, India